A Critical Review of Graphics for Subgroup Analyses in Clinical Trials and Some Improvements

Yi-Da Chiu[1‡], Nicolas Ballarini[2‡], Franz Koenig[2], Martin Posch[2] and Thomas Jaki[3*]

1. Royal Papworth Hospital NHS Foundation Trust, London, U.K. - MRC Biostatistics Unit University of Cambridge, School of Clinical Medicine, Cambridge, U.K.
2. Center for Medical Statistics, Informatics, and Intelligent Systems, Medical University of Vienna, Spitalgasse 23, 1090 Vienna, Austria.
3. Medical and Pharmaceutical Statistics Research Unit, Department of Mathematics and Statistics, Lancaster University, LA1 4YF, U.K.

‡These authors contributed equally to this work.

* t.jaki@lancaster.ac.uk

Abstract

Subgroup analyses are a routine part of clinical trials to investigate the effect of treatments in subsets of the population under study. The purpose of this assessment might be to ensure that there are no groups of patients for whom the treatment is harmful despite being effective in the majority of patients or to identify groups of patients that may benefit from a treatment when the overall effect is small or zero.

Graphical approaches play a key role in subgroup analyses to visualise effect sizes of subgroups, to aid the identification of groups that respond differentially, and to communicate the results to a wider audience. However, many existing approaches do not capture the core information and/or are prone to lead to a misinterpretation of the subgroup effects. In this work, we critically appraise existing visualisation techniques, propose useful extensions to increase their utility and attempt to develop an effective visualisation approach. The considered graphical techniques include level plots, contour plots, bar charts, Venn diagrams, tree plots, forest plots, Galbraith plots, L'Abbé plots, STEPP, alluvial plots, UpSet plots and chord diagrams. We illustrate the methods using a dataset of a treatment for prostate cancer.

Keywords: Data visualisation, treatment effect heterogeneity, personalised medicine.

1 Introduction

Investigating target populations that potentially benefit from an innovative intervention is essential in clinical trials. Even if efficacy is established in the overall population, a complete benefit/risk assessments of subgroups should be undertaken before deciding whether the treatment is administered to the whole population or certain subgroups need to be excluded [1]. Such investigations pose a challenge because of the various issues that are needed to address. For example, enrolling patients that have rather diverse baseline characteristics for considerations, such as age, gender, race, disease severity or biomarker profiles may create a large number of subgroups. The presence of promising results can be

attributed to small sample size or to the fact that many potential subgroups are explored, which affects the credibility level of the findings.

Subgroup analyses as investigative measures are prospective or post hoc in different settings of clinical trials. Their primary purpose can be to establish efficacy claims, subgroup discovery and/or consistency assessments across subgroups. Many researchers have proposed novel analysis approaches and designs for different types of subgroup analysis [2–4]. It has further received extensive attention in recent clinical research for the development of stratified medicine.

Visualisation techniques, when properly used, are powerful tools to reveal data. For example, it is argued that graphics, in most cases, allow a more direct interpretation than tables [5]. There is extensive literature in good statistical graphics principles in general (e.g. [6–12]) and in the health-care sector particularly [13–15]. However, it is also true that good graphics require careful crafting [16] and there is scope to improve when it comes to figures in clinical trial reports [17, 18].

Graphical approaches are routinely employed in subgroup analysis, typically for describing treatment effect sizes of subgroups. Such visualisations encapsulate subgroup information and boost the clinical decision-making process. However, not much attention has been paid to how to make effective graphics in the subgroup analysis setting. Existing approaches still have inherent drawbacks and their use may lead to misinterpretations on subgroup effect sizes [2]. For instance, forest plots, perhaps the most widely used graphics in the subgroup analysis setting, provide no insight into the overlap between subgroups. Additionally, whether or not a subgroup confidence interval crosses the no-effect point does not necessarily imply a differential effect in the subgroup. It is, therefore, crucial to correctly depict effect sizes and essential subgroups information.

In this paper, we attempt to develop an effective visualisation approach for subgroup analysis. Our considerations apply mainly to exploratory settings. The graphical techniques considered include level plots, mosaic plots, contour plots, bar charts, Venn diagrams, tree plots, forest plots, Galbraith plots, L'Abbé plots, STEPP, alluvial plots, UpSet plots, and chord diagrams. Some of these visualisations have been already proposed for subgroup analysis before (as the forest plots), some were improved in this work, and some techniques were developed for other applications and we show how they can be applied and/or extended for the visualisation of subgroups. To facilitate the discussion, we focus on a clinical trial dataset of a treatment for prostate cancer. All graphics are performed using the `R` statistical software [19] and the code is publicly available as an R package for reproducibility [20]. In most of the cases, we draw the plots using functions from the `grid` and `graphics` packages which are part of the base `R` language. However, for some of the plots, we use additional packages that are cited in each section accordingly.

Although we acknowledge that the choice of colours is an important and challenging task when producing graphics, we do not discuss this topic in our work, as there are other literature that already do it (see e.g [21, 22]). Several of the considered plots make use of colour coding to represent the magnitude of the treatment effect across subgroups, for which we use a divergent colour palette generated by the `colorspace` `R` package [23].

Another important aspect of graphics is human perception. We follow the principles by Tufte[24] to enhance graphical integrity. This is particularly relevant when we depict sample sizes with 2-dimensional areas/shapes which are proportional to 1-dimensional sample sizes. This is performed so that the representation of numbers are directly proportional to the numerical quantities represented.

The remainder of the paper is structured as follows: in Section 2 we describe the dataset we use for illustration and present the graphical approaches for displaying subgroup information. We put more emphasis on graphics that allow a direct comparison of

subgroup treatment effects (Section 2.1). We also present graphics that may complement the analysis providing an indirect comparison by displaying responses in treatment and control groups across subgroups (Section 2.2), and graphics that only allow visualising subgroup composition or overlap between subgroups (Section 2.3). Each technique is further assessed based on a set of criteria. We summarise the assessments and features of all approaches in Section 3. We remark their practical utility and implications in clinical trials and outline potential visualisation techniques in the end.

2 Graphical approaches to subgroup problems

It is fundamental that graphics in subgroup analysis display treatment effects for the subgroups under considerations. Nevertheless, there are also several other desirable characteristics for graphical approaches as initial subgroup analysis tools. Displaying sample sizes underpins the credibility level of promising and adverse findings within subgroups. It is also important to reveal overlap information, as this helps in clarifying that we look at the same signal several times and enables to focus on the subgroups that have less overlap with each other. The ability to detect treatment effect heterogeneity for subgroups and displaying the overall treatment effect should be considered as well. Moreover, it is expected that the graphic is available for a large number of subgroups to serve as a potential hypothesis generator. These characteristics can certainly constitute sensible criteria for assessment.

Our framework to assess the properties of the graphical displays consist of the following criteria:

C1 whether the plot displays effect sizes for subgroups;

C2 whether it exhibits subgroup sample sizes;

C3 whether it shows subgroups overlap information;

C4 whether it shows a measure of uncertainty of the treatment effect estimates in the subgroups (i.e. confidence intervals or standard errors);

C5 whether it is applicable to a large number of subgroup-defining covariates.

Each graphical approach is judged according to whether it meets each of the items or not. Even if a criterion is met, the information may be represented or encoded differently. For example, some graphics show the treatment effects in the subgroups using a colour scale while others represent them with the position along a common scale. Therefore, we discuss different levels of information in each of the graphics. We also discuss additional features, such as whether the graphics show the mean response in the treatment and control arms, what type of overlap they show, and the total number of subgroup-defining covariates that can be displayed.

We use a prostate carcinoma dataset from a clinical trial [25] which is available on the web [26]. The data has been used before to illustrate subgroup selection methods [27]. The first publication in which this data was used dates back to 1980, where authors already discussed methodology "to determine whether comparisons of treatment in various subsets of patients yield sufficiently different results to justify the idea that there may be an optimal treatment for each patient based on his individual characteristics" [25].

The trial included 506 subjects that were randomised to either a placebo group or one of three dose levels of diethylstilbestrol. For this study, we combine the placebo and

the lowest dose level of diethylstilbestrol to give the control arm, and the higher doses to give the experimental arm (as it was done in the previous referenced analyses). Only 475 subjects with complete data are available on the dataset. We are interested in identifying subgroups of patients that may benefit from the treatment. We consider only 6 pre-treatment covariates for this analysis, four of which are binary and two continuous: existence of bone metastasis (bm), disease stage (3 or 4), performance rating (pf: 0, normal; 1, limitation of activity), history of cardiovascular events (hx), age, and weight index (wt: weight in kg − height in cm + 200). In those plots that are more appropriate for only two binary/categorical factors, we use age and weight categorised into 3 levels for illustrative purposes (age: young=[48,65], middle-aged=(65,75], old=(75,89]; weight: low=[69,90], mid=(90,110], high=(110,152]), but a proper analysis of continuous covariates should treat them as continuous [28, 29]. When the plots are drawn using three covariates, we use only binary ones: existence of bone metastasis, performance rating and history of cardiovascular events. When the plots are drawn using four covariates, we added also the disease stage.

The original dataset includes information on causes of death. However, the considered endpoint in this analysis is death from all causes combined. Most of the graphical approaches we employ use the log-hazard ratio for treatment versus control as the treatment effect measure. For bar charts and L'abbé plots, we consider the difference in restricted mean survival time (RMST) as the treatment effect measure. In the case of bar charts, this is mainly to improve the interpretability. In the case of L'abbé plots, this is because the graphic requires not only a relative measure of the treatment effect but also an estimate for the response in control and treatment arms. In Section 2.2, we also use the two-year survival rate to exemplify graphical approaches with an indirect comparison of treatment effects that are better suited to binary outcome variables.

In most of the graphics, the treatment effect is estimated by simply partitioning the dataset and using only subjects from the considered subgroups. We acknowledge that this is perhaps not the best approach for obtaining treatment effect estimates and a proper analysis should be based on treatment-by-covariate interactions [30]. However, we choose to do this to focus on the graphical aspects rather than on the methodology to obtain the treatment effect estimates. Readers interested in techniques for obtaining treatment effect estimates in subgroups are referred to [4, 31, 32]. In any case, the graphics evaluated in this manuscript can be used to display the treatment effect estimates resulting from suitable models, which in turn may depend on a case by case basis.

2.1 Graphical approaches with a direct comparison of treatment effects

In this section, we devise graphics that represent or provide a measure of the treatment effect (e.g. hazard ratio) and therefore allow direct comparison across subgroups.

2.1.1 Level plot

Level plots are typically used to show geographic surfaces in a plane. In the subgroup analysis setting, two categorical variables are arranged on the axes, and the main plot area consists of cells that represent disjoint subgroups. Each subgroup is defined by the corresponding combination of levels of both covariates and a colour scale is used to display the treatment effect in that subgroup. In Figure 1a, we show the implementation of a level plot for treatment effect in terms of log-hazard ratios in subgroups defined by the categorised age and weight for the prostate cancer dataset. For each subgroup, a

Cox proportional hazards model with treatment as the independent variable is fitted to obtain the estimate for the hazard ratio. Alternatively, a single multivariate model with treatment by subgroup interactions may be fitted to obtain the estimates. A divergent colour scale with a range from -3 to 3 is used to represent the log-hazard ratio. We also add the point estimate and confidence interval for the overall population in the legend as a reference. We include the subgroups' sample sizes inside the cells. The cells on the bottom and the left margins represent the marginal subgroups corresponding to each of the three levels of age and weight, respectively.

This graphical approach is attractive since it permits a direct and easy interpretation of effect sizes, therefore satisfying criterion C1. A quick look at the colours allows drawing conclusions such as for which subgroups the treatment is beneficial and for which ones it is harmful. However, the variability of the subgroup estimates is not represented in this plot (C4), therefore making in it impractical to detect treatment effect heterogeneity. Although the addition of the sample sizes in the cells allows a comparison of the subgroup sizes, the sample sizes are not represented by the figure, therefore this display meets criterion C2 partially. Level plots may only display the pairwise overlay of marginal subgroups rather than all overlap across subgroups. It is worth noting that only two covariates can be considered in a level plot. The number of categories of each covariate can be easily ten (therefore, the number of subgroups can reach to a hundred), but this may lead to small subgroup sample sizes or even empty subgroups. Finally, we remind that because the cut-off points for continuous covariates may be arbitrary, level plots are better suited for categorical ones.

Examining Figure 1, we may conclude that the treatment is worse for older patients and young patients with low weight, as the direction of the treatment effect is reversed. Moreover, the treatment seems to be even more beneficial for heavier young patients. However, these interpretations need to be taken with care, as the precision of the estimates is not given and the small sample sizes in some subgroups may lead to highly variable estimates.

As a possible improvement, the coloured squares inside each cell are drawn with areas proportional to the subgroup sample sizes (Figure 1b). This design feature allows comparing subgroup sample sizes easily. At the same time, it may be difficult to see the colour in each square, particularly in the case of small sample sizes. Perhaps a better way to present the information of the level plot is using a mosaic plot as described in the following section.

[Figure 1 about here.]

2.1.2 Mosaic Plot

Mosaic plots are useful to represent contingency tables by arranging proportional-to-size cells in a grid. There are a number of variations in which this type of plot may be used in subgroup analysis. First, we devise an improvement of the level plot as in Figure 2a. Although the sample size annotation in each mosaic could be easily added, we omit it here as the sample sizes are depicted through the area of the mosaics. The interpretation of this plot is similar to the level plot presented in Figure 1b.

Mosaic plots offer the advantage that a larger number of covariates can be arranged. In Figure 2b, we use history of cardiovascular events, performance and bone metastasis to illustrate a mosaic plot with three subgroup-defining covariates. When adding additional covariates, however, it is not possible to show the information on marginal subgroups as in Figure 2a.

Figure 2b allows us to observe that there may be heterogeneity in the treatment effect as some subgroups have estimates on the positive direction while others on the negative one. However, the absence of uncertainty measures for the treatment effects estimates does not allow one making a conclusive interpretation.

[Figure 2 about here.]

2.1.3 Contour plot

An alternative to a level plot that is more suitable for illustrating continuous changes in relevant factors is a contour plot. We propose two different implementations of contour plots for the treatment effects across age and weight.

In Figure 3a, we first form subgroups with a specified sample size by neighbouring subjects in terms of their values of age and weight. Subgroups of sample sizes N_{11} are formed by using a sliding window across the values of age with an overlap of N_{12} subjects. Subsequently, each subgroup is further divided into smaller subgroups of sample sizes N_{21}, using again sliding window with an overlap of N_{22}. Sample sizes and overlap to form subgroups are adopted by design based on sensible judgement. For example, subgroups should have a considerable sample size to ensure that patients in both treatment and control arms are represented. For each formed subgroup, we then calculate the log-hazard ratio for treatment versus control. The contour areas are obtained through a bivariate interpolation and smooth surface fitting (loess) for irregularly distributed data points over the range of values from the subjects under study. We also use a divergent colour scale for the effect sizes. A limitation of this approach is that there may be regions of the covariate space in which the treatment effect estimates are not reliable due to small sample sizes or no data points.

We also propose using local regression techniques to calculate the treatment effect at each coordinate. In Figure 3b, a weighted Cox proportional-hazards model is fitted at each combination of weight and age (using a step of 1 unit). A normal kernel with the centre at the coordinate values under consideration is used to assign weights to each subject. If there are less than 20 subjects within 2 standard deviations, the effect size is not calculated and the area is left blank. This helps to avoid extrapolating the results to areas in which we do not have enough information.

According to our assessment, contour plots match criteria C1 and C3 but not C2, C4 and C5. Contour plots use two covariates and the total number of subgroups can be more than ten by controlling the overlap proportions with neighbouring subgroups. However, there is no graphical representation about subgroup sample sizes and uncertainty on the treatment effect estimates.

There are a few more noticeable characteristics for this graphical technique. Contour plots are particularly useful when a dataset size is rather large and for variables well distributed over the covariate range. Moreover, the interpolated effect sizes may be unreliable in the regions where there are no data points or only sparse points are irregularly distributed. In situations where the values of two covariates are sparsely distributed over the region, it may be unclear how smooth the interpolated surface should be. Note that it may also be possible to use other local regression algorithms to calculate the treatment effect at each coordinate or even other modelling strategies such as including a generalised additive model with interactions (such as in [28]). Recent proposals that investigate the predicted individual treatment effect can be applied to predict the effect of treatment across the covariate space [33–35].

We observe a similar pattern to the one found in Figure 1, in which the older patients seem not to benefit from the new treatment. Again, this interpretation should be cautious as the precision of the estimates is not displayed.

[Figure 3 about here.]

2.1.4 Venn diagram

Venn diagrams are undoubtedly the most widely used tool to visualise sets and their relations. In the subgroup analysis setting, Venn diagrams may be used to display the composition of a dataset. A Venn diagram for subgroups defined by bone metastasis, history of cardiovascular events and performance is shown in Figure 4a. Each circle defines the subgroup of patients for which the level of the corresponding variable is "yes" or 1. The diagram indicates the sample sizes for all the subsets that are formed by set operations (intersection and complement) on the three subgroup-defining covariates. The number outside of the three circles indicates the size of the complement of the union of the three subgroups.

[Figure 4 about here.]

Figure 4b and 4c consider Venn diagrams with four and three subgroup-defining covariates, respectively. Both encode the treatment effect in terms of the log-hazard ratio by colouring the corresponding regions. This feature thus enables the Venn diagram to satisfy the criterion C1. However, the variability of the estimates is not given and, therefore, C4 is not met.

As seen in Figure 4b, using four ellipses for representing all possible subgroups (formed through intersection and complement) is visually appropriate. Other shapes (such as polygons [36, 37]) can be also applied but the visualisations may not be easy to understand. In our example, however, we obtain subgroups with small sample sizes when considering the intersections of the four covariates. The white regions indicate that it is not possible to calculate the treatment effect in the corresponding subgroup. An additional rule may be added to this plot to colour only the areas that attain a pre-specified sample size.

Figure 4c further considers proportional-area methods, where each covariate representative region area is proportional to the respective sample size proportion. The region areas only approximately correspond the sample size proportions because of the limited degrees of freedom for circles. We employ the simple algorithm mentioned in [38]. In fact, other algorithms to display each region area proportional the sample sizes are available. Recently an algorithm that can produce accurate area-proportional Venn diagrams using ellipses was developed [38]. However, the algorithm is somewhat sophisticated and can only work on three sets.

Venn diagrams are implemented using the `VennDiagram` `R` package [39] together with the `polyclip` package [40]. For propotional-area Venn diagrams, we further use the `sp` package [41] and the `rgeos` package [42].

Venn diagrams satisfy C2, C3 in our assessment. Useful extensions to Venn diagrams, such as the Edwards' construction [43, 44], are available so that they can accommodate a larger number of covariates. The total number of subgroups including mutual disjoint ones can be 2^p, where p is the number of sets considered. Despite this merit, there is a limit on the number of the sets considered in practice. It may become complicated to interpret a Venn diagram with more than five subgroup-defining covariates.

Figure 4 shows that the treatment effect is reversed, with the control treatment being better than the experimental one for those subjects without bone metastasis when they have previous cardiovascular events or limitation of activity (performance rating is 1).

2.1.5 Bar chart

Another useful graphical technique to depict treatment effect sizes is bar charts. Bar charts are easy to interpret and allow direct comparison among subgroups. For the subgroup analysis problem, we use subgroups defined by the levels of categorised age and weight variables as in previous examples. In Figure 5, each covariate is categorised into three levels and the bars represent mutually disjoint subgroups. The levels of age and weight are respectively listed at the top and the bottom part of the picture. The height of the bars is proportional to the treatment effect differences between the experimental and control arms, that is, the difference in RMST. The width of the bars is proportional to the subgroup sample sizes. This arrangement has, therefore, another useful property: the area of the bars is proportional to the restricted mean survival gain or loss in each subgroup when using the experimental treatment in comparison to control. Different variations of grey were used to show which subgroups have the same category level on age.

Based on our assessment, this graphical representation approach holds C1 and C2, partially C3 but not C4 and C5. Each bar is the pairwise overlap of two subgroups defined by age and weight with their respective levels. Therefore, bar charts only provide partial overlay information. Such a graphical approach does not allow to examine heterogeneity in treatment effect differences across subgroups due to no display of the overall effect size.

Few noteworthy characteristics also need to be mentioned. First, it only considers two subgroup-defining covariates. If considering few more covariates, one could label all the level combinations of the covariates in the bottom part of the picture or simply to make a legend elsewhere. However, a high number of covariates or levels may be problematic, making it difficult to compare the widths of the bars. Second, as in level plots, the cut-off points for categories in continuous variables may be arbitrary and categorical covariates are therefore preferred for bar plots.

Although we use a different measure for the treatment effect, the direction of the estimates is maintained compared to the level plot in Figure 1 and the interpretation remains unchanged.

[Figure 5 about here.]

2.1.6 Forest plot

Although forest plots are a common graphical display approach for meta-analysis [45], they are also extensively used for subgroup analysis [46, 47]. In a forest plot, the treatment effect estimates along with their confidence intervals for the subgroups defined by a number of covariates are displayed vertically. The overall treatment effect is also plotted on top allowing a direct comparison. It is also suggested that a vertical line at the overall treatment effect level is added to facilitate seeing if a subgroup confidence interval differs significantly from the overall effect [46]. Figure 6 shows its application for the prostate cancer dataset considering four binary covariates. The main panel in the middle displays the subgroup treatment effects with their confidence intervals. The squares in the centre of each error bar are proportional to the subgroup sample sizes. Additional information in a table format is usually included to provide the exact magnitude of the

estimates. The text on the left panel shows the mean estimate of treatment effect difference, lower/upper bounds of the 95% confidence intervals and subgroup sample sizes (further divided into treatment and control arms). When using a continuous or binary endpoint, it is also recommended to include the estimates for treatment and control to observe whether both interventions have harmful effects despite the promising effect size. In our implementation for survival endpoint, we include the Kaplan-Meier curves for each subgroup. The summary statistics on the panel on the left and the survival curves on the right may, however, be dropped if needed. The Kaplan-Meier curves are drawn with the `ggplot2` package [48].

From the above description, forest plots in the subgroup analysis setting meet all the criteria but C3 because of the inability to show subgroup overlaps.

We observe in Figure 6 that the subgroup with bone metastasis is the subgroup with the largest benefit from the treatment, while for the rest of the subgroups their treatment effect is closer to that on the overall population. The Kaplan-Meier curves allow to rapidly recognise the differential survival pattern for the subgroup with bone metastasis.

[Figure 6 about here.]

2.1.7 Tree plot

The tree plot for subgroup analysis starts with the full population that branches into two or more items, corresponding to the levels of the first subgroup-defining covariate. Each of the items in the new level branch again into two or more levels for the second covariates, then for the third and so on. If more variables were included, this division procedure is consecutively conducted to form subgroups until all the category combinations of the covariates are considered. Figure 7 shows a tree plot of treatment effect differences for subgroups defined by bone metastasis, performance rating and history of cardiovascular events. In each level or layer, treatment effect differences and their 95% confidence intervals for the associated subgroups are also displayed. The purple horizontal lines placed in the middle of the confidence intervals have a length proportional to the subgroup sample sizes. An additional horizontal dotted line is added at each level for the overall treatment effect size. In Figure 7a, the y-axis for each level of the plot is drawn independently from the others levels. In the Figure 7b, the y-axes are consistent across levels, which helps to visualise the difference in variability of the estimates.

Tree plots match all the criteria. It obviously fit meets C1 and C2 by design. In addition, the subgroups at each layer are formed by the intersection of the levels of the covariate in that layer with the covariates that are placed above them, thus holds C3 for displaying the information of all subgroup overlaps. Moreover, the confidence intervals for treatment effect estimates in subgroups are displayed, fulfilling C4. Similar to forest plots, the assessment of treatment effect heterogeneity demands drawing an auxiliary horizontal line with the y-coordinate at the overall effect size for each layer and then seeing whether there is any confidence interval not crossing the line. As to C5, it may be difficult to arrange a large number of covariates in tree plots. However, note that the total number of subgroups depends on the number of covariates that are involved and how many categories each covariate has.

It is worth pointing out a few features of tree plots. First, it provides information on the interval estimation for subgroup effect sizes. Second, it is possible to consider more than two categories for each covariate if needed. Ideally, however, the number of covariates and categories should be moderate or we may end up with subgroups small sample sizes. Finally, when considering continuous covariates tree plots have the same

issue about arbitrary cut-off points as level plots and bar charts. In this implementation, the ordering of the covariates needs to be pre-specified. Recent proposals that allow the data to define the ordering and/or cutoff values for continuous variables [49, 50] can also be used to draw tree plots.

Figure 7 allows us to draw additional conclusions regarding the treatment effect sizes. We observe that the treatment effect is more pronounced for subjects with bone metastasis. Additionally, we notice that the subgroup of subjects without bone metastasis but with a history of cardiovascular event and performance rating 1 has a positive log-hazard ratio, implying that the control is better than the experimental treatment for this subgroup.

[Figure 7 about here.]

2.1.8 Galbraith plot

A Galbraith plot [51, 52] is an alternative or supplementary to a forest plot for examining heterogeneity of studies or subgroups in a meta-analysis. The variant that is shown in Figure 8 exhibits the estimation of treatment effect sizes for $K = 8$ subgroups defined by the four binary covariates. The xy-coordinates correspond to the points:

$$x_i = 1/\sqrt{\hat{\text{Var}}(\hat{\delta}_i)}, \quad y_i = (\hat{\delta}_i - \hat{\delta}_F)/\sqrt{\hat{\text{Var}}(\hat{\delta}_i)} \tag{1}$$

where $\hat{\delta}_F$ is the treatment effect estimate in the full population and $\hat{\delta}_i$ is the treatment effect estimate in subgroup i, $i = 1, ..., K$. The grey band serves to detect treatment effect heterogeneity if one point is located outside the band. The slope of the line from the origin through each subgroup point corresponds to the effect size estimate $\hat{\delta}_i$ of the corresponding subgroup. An additional radial axis is drawn to depict the subgroup effect sizes, which are represented with the red tick marks. The central line at $y = 0$ points to the average treatment effect for the full population.

We note here that, as $\hat{\delta}_F$ is itself a random variable, it may better to consider also its variance. An additional modification may then consider the xy-coordinates:

$$x_i = 1/\sqrt{\text{Var}(\hat{\delta}_i - \hat{\delta}_F)}, \quad y_i = (\hat{\delta}_i - \hat{\delta}_F)/\sqrt{\text{Var}(\hat{\delta}_i - \hat{\delta}_F)}$$

The resulting plot using such these values is given in the Supplementary Material. The drawback of this modification is that the x-axis does no longer represent the standard error of the treatment effect estimates.

The result of the graphical assessment of Galbraith plots is satisfactory. It obviously holds C1, C4 and C5 because of its design features. Galbraith plots can certainly handle a large number of subgroup covariates, perhaps better than any of the other considered graphics. The Galbraith plot does not show the sample sizes of the subgroups. Moreover, it does not hold C3 as it does not display subgroup overlap information.

In terms of our example, we conclude that treatment effect heterogeneity may be present in the subgroup of patients with bone metastasis.

[Figure 8 about here.]

2.1.9 L'Abbé plot

L'Abbé plots [53] are a variant of scatter plots which are useful for examining heterogeneity in a meta-analysis. The graphical design is originally for binary outcome data to represent risk ratios, risk differences or odds ratios between treatment and control arms. For our implementation, we extend this graphical technique to the case of continuous and survival outcomes and also modify points to rectangles (Figure 9). The $xy-$coordinates for each subgroup correspond to the estimates of the RMST in control and treatment arms. The width and the height of a rectangle (corresponding to a subgroup) respectively indicate the sample sizes of the control and experimental treatment arms in the subgroup. We draw a diagonal dashed line at $y = x$ which represents no treatment effect (equal RMST in both arms) and a solid diagonal line with y-intercept at the overall treatment effect size. Each rectangle has a vertical segment from its centre to the diagonal dash line representing the magnitude of the effect size, that is the gain (if blue) or loss (if red) in terms of RMST when comparing treatment vs. control.

L'Abbé plots satisfy C1, C2, and C5; but they do not show the uncertainty of the treatment effect estimates nor show subgroup overlap information. While they may handle many subgroups, it may be difficult to recognise the corresponding rectangles if subgroups have a similar effect estimate for treatment and control groups.

This graphical tool allows us to draw an additional conclusion in our example. The subjects with bone metastasis in the control group have a lower RMST compared to other subgroups. When receiving the experimental treatment, however, the RMST is closer to that on the other subgroups.

[Figure 9 about here.]

2.1.10 STEPP

The subpopulation treatment effect pattern plot (STEPP) [54, 55] gained popularity in breast cancer recently. It is a non-parametric method mainly for examining whether treatment-covariate interactions exist. In Figure 10, we adopted the slide-window fashion of STEPP to represent the estimation of treatment effect size (log-hazard ratio) in overlapping subgroups defined by age. Each subgroup has a sample size of around 40 with about 80% overlap with neighbouring subgroups. The band bounded by the blue dashed lines is constructed for 95% simultaneous confidence interval. The other band bounded by the orange dashed lines is built based on individual 95% C.I. (without multiplicity adjustment). The red line is formed by connecting the point estimates of treatment effect (log-hazard ratio) for all formed subgroups. The green line represents the log-hazard ratio estimate for the full patient population. It is worth noting that the point estimates are positioned at the mean value of age for each subgroup with respect to the $x-$axis. If the green line does not lie in the region formed by simultaneous confidence intervals, it reveals that interaction may exist.

The STEPP approach matches C1, C3 and C4. Here, the information about subgroup overlap and sample sizes is only annotated in the figure and the caption. It is noted that, although only one subgroup-defining covariate is used, the total number of subgroups depends on the sample size of subgroups and the overlap proportions.

This plot only considers one continuous covariate. It is difficult to extend the application for more continuous covariates. The subgroup sample sizes should be specified by design, and in some situations, a researcher may have no clear idea about how large a subgroup should be and how much it should overlap with the immediate subgroups.

Perhaps, practitioners need to conduct sensitivity analyses for different subgroup sample sizes and overlaps. The analysis results may further be compared with the results when using fractional polynomials [28, 56] or non-parametric methods (such as Gaussian processes [57]).

For our example, we observe that the treatment effect for subgroups defined by age fluctuates around the overall treatment effect. When approaching the ends of the range of the covariate the estimate of the log-hazard ratio departs from the estimate for the full population, although the confidence intervals still cover it.

[Figure 10 about here.]

2.1.11 UpSet Plot

UpSet plots are a novel visualisation technique for the quantitative analysis of sets and their intersections [58]. It was proposed to overcome the limitation of Venn diagrams of showing up to a small number of sets or subgroup-defining covariates. In Figure 11, we use the `UpSetR` R package [59] to create the plot with the six subgroup-defining covariates. The variable age is dichotomized (1: >75 years), as is weight (1: >100) to have binary covariates. The sizes of the univariate subgroups for these covariates are shown in the horizontal bar plot at the bottom-left corner of the figure. The "matrix" layout on the bottom allows visualising the composition of the subgroup by showing which sets are intersected. The main bar plot displays the sizes of the subgroups that are defined by the respective intersections. For example. the first and tallest bar indicates there are 52 subjects with performance rating 0 (normal), no existence of bone metastases, age ≤ 75, weight > 100, disease stage 3, and no history of cardiovascular events. Moreover, we add a 'query' to display the frequency of treatment and control of each subset.

[Figure 11 about here.]

We extend the `UpSetR` R package to display effect sizes in an extra panel (Figure 12). In this case, the log-hazard ratio and its confidence interval for each subgroup are shown. This information is similar to that in the forest plots. However, the UpSet plot provides the advantage to observe intersection of sets and arrange them in terms of their sizes. If one were to use a statistical model with treatment-by-covariate interactions to derive the treatment effect estimates, then each row would correspond to a linear combination of the coefficients in the model.

Our extension of the UpSet plot also allows displaying lower level intersections. We implement a new icon for the matrix panel: a '+' symbol if a variable is equal to 1 or 'yes', a '-' if a variable is equal to 0 or 'no', and empty if this variable is not considered for the subgroup definition. For example, the first bar of the plot corresponds to the overall population (no subgroup division), which has a size of 475. The second bar with a size of 428 corresponds to the subgroup of normal performance rating (pf=0), irrespective of the values of the other two variables. Since the number of subgroups to consider increases dramatically in this modification (3^p subgroups when considering p binary covariates), only three covariates are considered. One can include, however, more covariates and filter the number of subgroups according to different criteria, such as total subgroup sample size, sample size per treatment, etc. Finally, the bar plot on top of the matrix panel indicates the marginal set sizes in relation to the total sample size, with the black region corresponding to the 1 or 'yes' category and the white region corresponding to the 0 or 'no' category.

The modified UpSet plot meets all criteria. Its advantage is that it is scalable, and thus allowing a large number of subgroup-defining covariates. As the overall treatment effect and its confidence interval are also included in this modification, it allows to compare treatment effects and check for treatment effect heterogeneity.

[Figure 12 about here.]

2.1.12 Chord Diagram

Chord diagrams are widely used to visualise genomic data [60]. There are several approaches to these diagrams, although the main aspect is that it allows representing the relationships between pairs of sets. For our example, we use the categorised variables age and weight (Figure 13). The categories of each variable are arranged along the circle, where each of their corresponding cells has a size proportional to the corresponding subgroup sample size and a colour representing the treatment effect estimate, in terms of the log-hazard ratio. The ribbons on the centre of the diagram represent the relative overlap between the categories of the variables. Their width is calculated in correspondence to the proportion of subjects from a subgroup that is also in the subgroup to which the bands connect. We implement this graphic using the `circlize` R Package [61].

Chord diagrams meet all the criteria but C4 since they do not display any uncertainty measures of the treatment effect estimates. The flexibility of this plot is also an advantage since many other implementations may be devised, especially when the number of covariates is extremely large as when dealing with genomic data.

Figure 13 allows us to observe the treatment effects across the subgroups defined by age and weight marginally. Since the direction of the treatment effect changes across the levels of the age covariate, treatment effect heterogeneity may be present. Again, using a colour scale and not displaying variability estimates hinders a definite conclusion.

[Figure 13 about here.]

2.2 Graphical approaches with an indirect comparison of treatment effects

In some cases, it may be also of interest to visualise responses by treatment arm across subgroups. For example, we may want to display the survival or mortality rate, or simply the mean response if a continuous endpoint is considered. The following plots that we consider are examples of graphics that allow an indirect comparison of treatment effects.

2.2.1 Mosaic Plot

We could use mosaic plots to illustrate event rates per treatment group across the levels of one subgroup-defining covariate, as it is used in [11]. This plot is only appropriate when the endpoint is binary, therefore we use 2-year survival (blue corresponds to 'yes') by treatment and age category (Figure 14). In this case, it is possible to observe that the survival rate is larger for treatment in the younger patients while the survival rate is larger for control in the older patients, indicating that the treatment effect may not be homogeneous across the levels of age.

[Figure 14 about here.]

2.2.2 Coxcomb plot (Nightingale rose)

A Nightingale coxcomb plot [62] is a type of radial plot that was introduced in 1858 and is usually recommended as an alternative to pie charts [9]. In Figure 15, we arrange the subgroups defined by the categorised age and weight variables along the circle using a combination of bar plot and polar coordinates with the `ggplot2` `R` package. In this plot, the angles that define each sector are kept fixed, but the radii vary proportionally to the square root of the sample size in each subgroup to perceive areas adequately. We colour the areas according to the 2-year survival rate of each subgroup.

In Figure 16, we further divide the plot into treatment and controls arms. This feature allows us to check the sample sizes per subgroup in each treatment arm and may help visualise differences in the survival rates.

[Figure 15 about here.]

[Figure 16 about here.]

2.2.3 Alluvial diagram

Alluvial diagrams are flow diagrams that can be used to display the distribution of the subjects across the subgroup-defining covariates. As the mosaic plots, alluvial diagrams may also be used to illustrate event rates per treatment group across the levels of the subgroup-defining covariate.

Figure 17 shows one possible implementation of the alluvial plot for the 2-year survival per treatment arm across levels of performance, history of cardiovascular events and bone metastasis. The plot is generated using the `alluvial` R package [63].

Alluvial diagrams do not provide any information regarding treatment effect sizes, but only on the composition of the subgroups, meeting criteria C2 and C3 as Venn diagrams. Alluvial diagrams can also display a large number of subgroups and can be used not only with binary covariates but also categorical ones. When the covariates are continuous, however, parallel coordinates plots can be used in a similar way.

[Figure 17 about here.]

2.3 Graphical approaches for subgroup composition

Figure 18 shows another implementation of alluvial plots for subgroup composition. The blue coloured bands correspond to patients that were randomised to treatment while light-blue bands to patients in control. The height of the bars for each category in the subgroup-defining covariates is proportional to the numbers of subjects in this category, therefore giving a notion of the size of the subgroup. Each alluvium (or band) represents the combination of values for the covariates. Therefore this diagram has also the advantage of giving an idea of the overlap of the subgroups, via the width of the bands.

[Figure 18 about here.]

Forest plots, Galbraith plots and L'Abbé plots share the inability of showing subgroup overlaps. One potential improvement is to consider combining relevant figures about overlap information.

The plots that are shown in Figure 19 exhibit subgroup information about pairwise overlap proportions or similarity measures. Figures 19a- 19d show pairwise relative overlap proportions, where colours encode the overlap magnitudes. All plots are generated using the `graphics` `R` package, while we also make use of the `diagram` package [64] for some of them.

More specifically, Figure 19a is a plot with bidirectional arrowed curves. The subgroup positioned at the starting point of each arrow is used as a baseline for calculating the relative proportion of the overlapping subgroup. Figure 19b is a variant of Figure 19a. Two identical sets of subgroup labels around two circles and each shows relative overlapping proportions with unidirectional arrowed coloured lines. The subgroup labelled at the starting point of the arrowed line is a baseline subgroup for the relative overlapping proportion. Figure 19c is a plot merely using coloured lines connecting subgroup labels on different levels. This plot should be read from top to bottom. A subgroup label on the higher level is the baseline subgroup for the relative overlapping proportions with its counterpart on the lower level. Figure 19d is a matrix plot for relative overlapping proportions of pairwise subgroups. The row subgroup label indexes what subgroup should be considered as a baseline and the sizes of the circles signal the overlap magnitude.

Both Figures 19e-19f show dissimilarity distance, which is defined by one minus a relative overlap proportion. Each line of Figure 19e shows the dissimilarity distance of a subgroup with the others. The red crosses along each line are located according to actual dissimilarity distances; the red subgroup labels correspond to the red crosses, where the labels are placed by order based on their actual dissimilarity distances. Figure 19f shows the same information as Figure 19e. Note that for each subgroup we do not show its dissimilarity distance to itself and its complement.

Incidentally, the Jaccard index, namely $|A \cap B|/|A \cup B|$ for any sets A, B, can replace the pairwise overlap proportions for subgroup overlap information. The graphical display is thus simplified due to not showing repetitive Jaccard indexes. However, this measure may lead to missing some information about whether a subgroup contains the others or not.

In the Supplementary Material, we present additional alternatives for the line and chord diagrams that display the overlap between the subgroups using a matrix layout. These plots may be easier to interpret as they are not overloaded with information and one can focus on one subgroup at the time. However, these plots may be impractical when having a large number of subgroups.

[Figure 19 about here.]

2.4 Subgroup analysis conclusion

The true test of a graphic is what information you can gain from it. Throughout the manuscript, we explored the prostate cancer dataset to find promising subgroups. Here we present an overall summary of the main findings related to subgroups.

In the Forest plot (Figure 7), we explored the treatment effects for subgroups defined by binary covariates marginally. The treatment effect was similar across all subgroups but in one of the patients with bone metastasis. We can detect that patients with bone metastasis seem to have an extra benefit from the experimental treatment because the confidence interval for this subgroup does not cover the line that represents the treatment effect in the overall population. The same trend is observed when using a Galbraith plot (Figure 9), as we see that the only point lying outside the (-2, 2) band is the one corresponding to the subgroup of patients with bone metastasis. When using the

difference in RSMT in the L'abbé plot (Figure 10), we also observe that the line from the centre of the polygon corresponding to the subgroup of patients with bone metastasis to the y=x line is much larger than the one for the full population.

The Figures 5, 8 and 12 also explored the binary covariates, allowing one to draw additional conclusions as the subgroups formed by the set intersections are also displayed. For example, the tree plot also shows the differential effect of the subgroup with bone metastasis, but also shows that this trend is only observed in patients who additionally do not have a history of cardiovascular events. Moreover, it may also be observed that patients without bone metastasis and with a history of cardiovascular events may have been harmed by the experimental treatment.

The variables age and weight were explored in Figures 1, 3, 10, 19. In all these figures we observed that the treatment seems more beneficial for younger patients with weight index above 90, while for older patients the treatment may have led higher hazard. This same trend can also be seen in the mosaic plot for the 2-year survival time by age group and treatment (Figure 14), where we observe a higher survival rate in the experimental group compared to the control one in the younger patients, but a higher survival rate for the patients in the control group in among the old patients.

We remind here, however, that these analyses are exploratory and should be taken with care. They may, however, bring useful insights to plan additional studies and collect more information from subgroups of interest.

3 Discussions and conclusion

We made use of several graphical approaches and assessed their characteristics for subgroup problems. We also attempted to improve some methods by mitigating their demerits. The assessment and characteristics of the improved approaches are summarised in Table 1.

The general summary is as follows:

C1, Effect sizes for subgroups: This information is encoded in different ways across the studied graphics. Research on graphical perception suggests that quantitative reasoning is trivial when encoding the information with the position on a common scale (such as in forest plots, UpSet plots, Galbraith plots and L'abbé plots); but requires more effort when it is encoded on colour hue or saturation (such as in level plots, mosaic plots, contour plots and Venn diagrams) [65]. Therefore, even if most of the graphical techniques satisfy the primary criterion of displaying subgroup effect sizes, some may be more effective at communicating the results from the analysis than others. Additionally, forest plot and L'Abbé plot also provide subgroup responses for the treatment and control arms.

C2, Subgroup sample sizes: The majority of the approaches provide a visual display on subgroup sample sizes. Some of the graphics achieve this criterion by encoding the subgroup sample size information in areas (level plots, mosaic plots, Venn diagrams), while others display the actual sample size number on the graphic. A notable approach here is the UpSet plot, which displays the subgroup sample sizes in an additional panel using a barplot. While one can add an additional barplot showing sample sizes to any of the other graphics, the particular assembly of the UpSet plot is optimised to decode the information quickly and efficiently.

C3, Subgroup overlap information: The third criterion is fully or partially met for all apart from Forest plots, Galbraith plots and L'abbé plots. Venn diagrams, tree plots, and UpSet are able to show the overlay of all subgroups. The remaining approaches only display the pairwise overlap of subgroups. It is noted that when the number of subgroups

Table 1: The assessment summary of graphical techniques for subgroup problems. The assessment criteria are: **C1**: whether the plot displays effect sizes for subgroups; **C2**: whether it exhibits subgroup sample sizes; **C3**: whether it shows subgroups overlap information; **C4**: whether it shows a measure of uncertainty of the treatment effect estimates in the subgroups (i.e. confidence intervals or standard errors); **C5**: whether it is applicable to a large number of subgroup defining covariates. The overlap column corresponds to P: pairwise overlap or A: all overlap. N_c represents the number of covariates for considerations

	Criterion					Additional features		
	C1	C2	C3	C4	C5	T/C Effect	Overlap	N_c
Level plot	✓	✓	✓				P	2
Mosaic plot	✓	✓	✓				P	2-10
Contour plot	✓		✓				P	2
Venn diagram*	✓	✓	✓				A	2-6
Bar chart	✓	✓	✓				P	1-5
Tree plot	✓	✓	✓	✓			A	1-5
Forest plot*	✓	✓		✓	✓	✓		1-40
Galbraith plot*	✓			✓	✓			1-100
L'Abbé plot*	✓	✓			✓	✓		1-40
STEPP	✓		✓	✓			P	1
UpSet plot*	✓	✓	✓	✓	✓		A	1-40
Chord diagram	✓	✓	✓		✓		A	2-100
Coxcomb plot		✓	✓			✓	A	1-5
Alluvial diagram		✓	✓			✓	A	1-10

*The plot has been improved or modified to make it available for the subgroup analysis framework

is small (say, up to five), the forest plot, Galbraith plot and L'Abbé plot can combine a Venn diagram or other plots for displaying overlap of subgroups.

C4, Measures of uncertainty of the treatment effect estimates: This characteristic is not present in all approaches. We issue a warning here since visualisations that do not adequately demonstrate the uncertainty of the estimates may be misleading and can lead to an over-interpretation of the heterogeneity of the treatment effect across subgroups. Some of the plots include a reference line corresponding to the overall effect size. The judgement of heterogeneity generally depends on the distances between the treatment effect estimate in the full population, the estimates in subgroups and their variability.

C5, Whether a large number of subgroup-defining covariates is possible: As for the last criterion, only five techniques (forest plots, Galbraith plots, L'Abbé plots, UpSet, and chord diagrams) may be available to handle more than ten subgroups-defining covariates. Venn diagrams and tree plots can practically deal with only up to five sets for effective visualisation.

In practice, the decision to use one technique or another demands the consideration of different characteristics and circumstances. For example, we have seen that contour plots and STEPP are only suitable for continuous covariates, while the rest allows the use of binary or categorical covariates. Level plots and bar charts may be easier to understand due to their simple design. Forest plots and L'Abbé plots can be used especially to identify subgroups with adverse effects in both interventions despite the positive effect size. As some graphics do not display key information, combining several ones may also be advantageous.

The approaches are worthy of further discussions in design and use issues. One thing to note is that the results of statistical inference based on hypothesis testing are not

informed. Our primary goal was to visualise essential subgroup information including effect sizes and sample sizes. We consider that all the approaches mainly serve as graphical descriptive tools, and therefore there is no need for adding the testing results for initial subgroup analyses. As a result, the presence of positive or adverse findings in subgroups with small sample sizes only brings concerns to practitioners for further investigations.

Related to this point, it is important to note that the considered graphical approaches are descriptive only and do not adjust for potential selection bias of point estimates, inflated type 1 errors due to multiple testing, or reduced simultaneous coverage probabilities of confidence intervals. These consequences of multiple testing and selective estimation may become, however, substantial as the number of considered subgroups increase. In exploratory settings though, where the definition and selection of subgroups are post hoc and may be data-driven, frequentist error rates or coverage probabilities cannot be controlled on principle. In contrast, if the subgroups to be considered are pre-defined (or selected independently of outcome data), there is a broad range of statistical approaches available to account for multiplicity [3, 66]. Many of the considered graphical approaches can be used to show multiplicity adjusted treatment effects and uncertainty measures. One can, for example, use simultaneous confidence intervals based on the Bonferroni correction, post-selection confidence intervals as in [35], treatment effects estimates after model averaging [67], bias-adjusted estimates [27], etc. Comparative plots showing both the adjusted and unadjusted estimates may also provide valuable insight.

Another issue is the correlation between categorical variables considered. The graphical approaches are not designed to address the problem that the correlation causes, where estimates from mutually disjoint subgroups can be correlated and thereby this may lead to confounding interpretations of subgroup effect sizes. This can be solved by using, for example, a standardisation technique before utilising the graphical approaches [68].

In this work, we focused on developing non-interactive graphical displays. We recognise the usefulness of adding interactivity, which can improve the flexibility of the studied graphics. For example, there exist work on interactive mosaic plots [69] which allows one to easily include more subgroup-defining covariates to avoid the problem of overlapping labelling. Interactive UpSet plots allow one including/excluding covariates, ordering them according to different characteristics, displaying additional variables, etc; which makes this graphic a powerful analysis tool (https://caleydo.org/tools/upset/). The recently published `subscreen` package [70] enables the analysis of thousands of subgroups by using a scatter plot and allowing the user to display additional information thanks to interactive tools like `R` Shiny [71]. Certainly, all graphics may benefit from interactivity. It appears to be feasible to adapt existing interactive approaches to the subgroup analysis problem or to add interactivity to the graphics that we introduced in this manuscript.

The dataset we analysed contained information on causes of death. However, the considered endpoint in the analysis in this manuscript was death from all causes combined. Additionally, while four treatment options were used to treat the patients, we combined them into two categories. These adaptations allowed us to frame the analysis in the typical situation where an experimental treatment is compared against a control. Modifications to the considered graphics could be explored to enable the comparison of multiple treatments or multiple endpoints. Again, interactivity may also help in these situations to explore and understand the data.

The code used to generate the figures in this manuscript is provided as an R package in the online supplementary material and is also available in CRAN (https://cran.r-project.org/package=SubgrPlots).

Acknowledgements

This project has received funding from the European Union's Horizon 2020 research and innovation programme under the Marie Sklodowska-Curie grant agreement No 633567. Prof Jaki's contribution is independent research arising in part from Prof Jaki's Senior Research Fellowship (NIHR-SRF-2015-08-001) supported by the National Institute for Health Research. Funding for this work was also provided by the Medical Research Council (MR/M005755/1). The views expressed in this publication are those of the authors and not necessarily those of the NHS, the National Institute for Health Research or the Department of Health.

References

[1] Committee for Medicinal Products for Human Use. Guideline on the investigation of subgroups in confirmatory clinical trials. *London: European Medicines Agency*, 2014.

[2] Mohamed Alosh, Mohammad F Huque, Frank Bretz, and Ralph B D'Agostino. Tutorial on statistical considerations on subgroup analysis in confirmatory clinical trials. *Statistics in medicine*, 36(8):1334–1360, 2017.

[3] Thomas Ondra, Alex Dmitrienko, Tim Friede, Alexandra Graf, Frank Miller, Nigel Stallard, and Martin Posch. Methods for identification and confirmation of targeted subgroups in clinical trials: a systematic review. *Journal of biopharmaceutical statistics*, 26(1):99–119, 2016.

[4] Alex Dmitrienko, Christoph Muysers, Arno Fritsch, and Ilya Lipkovich. General guidance on exploratory and confirmatory subgroup analysis in late-stage clinical trials. *Journal of biopharmaceutical statistics*, 26(1):71–98, 2016.

[5] Andrew Gelman, Cristian Pasarica, and Rahul Dodhia. Let's practice what we preach: turning tables into graphs. *The American Statistician*, 56(2):121–130, 2002.

[6] Edward R. Tufte. *The Visual Display of Quantitative Information.* Graphics Press, Cheshire, CT, USA, 1983.

[7] William S Cleveland. A model for studying display methods of statistical graphics. *Journal of Computational and Graphical Statistics*, 2(4):323–343, 1993.

[8] John W Tukey. *Exploratory data analysis*, volume 2. Reading, Mass., 1977.

[9] Naomi B Robbins. *Creating more effective graphs.* Wiley, 2012.

[10] Leland Wilkinson. *The grammar of graphics.* Springer Science & Business Media, 2006.

[11] Richard M Heiberger and Burt Holland. *Statistical analysis and data display: an intermediate course with examples in R.* Springer, 2015.

[12] Winston Chang. *R Graphics Cookbook: Practical Recipes for Visualizing Data.* " O'Reilly Media, Inc.", 2012.

[13] Milo A Puhan, Gerben Ter Riet, Klaus Eichler, Johann Steurer, and Lucas M Bachmann. More medical journals should inform their contributors about three key principles of graph construction. *Journal of clinical epidemiology*, 59(10):1017–e1, 2006.

[14] Andreas Krause and Michael OConnell. *A picture is worth a thousand tables: graphics in life sciences*. Springer Science & Business Media, 2012.

[15] Susan P Duke, Fabrice Bancken, Brenda Crowe, Mat Soukup, Taxiarchis Botsis, and Richard Forshee. Seeing is believing: good graphic design principles for medical research. *Statistics in medicine*, 34(22):3040–3059, 2015.

[16] Martin Krzywinski. Points of view: elements of visual style, 2013.

[17] Stuart J Pocock, Thomas G Travison, and Lisa M Wruck. Figures in clinical trial reports: current practice & scope for improvement. *Trials*, 8(1):36, 2007.

[18] Jennifer C Chen, Richelle J Cooper, Michael E McMullen, and David L Schriger. Graph quality in top medical journals. *Annals of emergency medicine*, 69(4):453–461, 2017.

[19] R Core Team. *R: A Language and Environment for Statistical Computing*. R Foundation for Statistical Computing, Vienna, Austria, 2017.

[20] Nicolas Ballarini and Yi-Da Chiu. *SubgrPlots: Graphical Displays for Subgroup Analysis in Clinical Trials*, 2018. R package version 0.1.0.

[21] Achim Zeileis, Kurt Hornik, and Paul Murrell. Escaping rgbland: selecting colors for statistical graphics. *Computational Statistics & Data Analysis*, 53(9):3259–3270, 2009.

[22] Mark Harrower and Cynthia A Brewer. Colorbrewer. org: an online tool for selecting colour schemes for maps. *The Cartographic Journal*, 40(1):27–37, 2003.

[23] Ross Ihaka, Paul Murrell, Kurt Hornik, Jason C. Fisher, and Achim Zeileis. *colorspace: Color Space Manipulation*, 2016. R package version 1.3-2.

[24] Edward Tufte and P Graves-Morris. The visual display of quantitative information.; 1983, 2014.

[25] David P. Byar and Sylvan B. Green. The choice of treatment for cancer patients based on covariate information: application to prostate cancer. *Bulletin du Cancer*, 67:477–490, 1980.

[26] Patrick Royston and Willi Sauerbrei. Multivariable model-building: Advanced prostate cancer dataset, 2008. Accessed: 2017-06-01.

[27] Gerd K Rosenkranz. Exploratory subgroup analysis in clinical trials by model selection. *Biometrical Journal*, 58(5):1217–1228, 2016.

[28] Patrick Royston and Willi Sauerbrei. A new approach to modelling interactions between treatment and continuous covariates in clinical trials by using fractional polynomials. *Statistics in medicine*, 23(16):2509–2525, 2004.

[29] Patrick Royston, Douglas G Altman, and Willi Sauerbrei. Dichotomizing continuous predictors in multiple regression: a bad idea. *Statistics in medicine*, 25(1):127–141, 2006.

[30] European Medicines Agency. Guideline on the investigation of subgroups in confirmatory clinical trials, 2014.

[31] Ilya Lipkovich, Alex Dmitrienko, and Ralph B D'Agostino Sr. Tutorial in biostatistics: data-driven subgroup identification and analysis in clinical trials. *Statistics in Medicine*, 36(1):136–196, 2017.

[32] Marius Thomas and Björn Bornkamp. Comparing approaches to treatment effect estimation for subgroups in clinical trials. *Statistics in Biopharmaceutical Research*, 9(2):160–171, 2017.

[33] Andrea Lamont, Michael D Lyons, Thomas Jaki, Elizabeth Stuart, Daniel J Feaster, Kukatharmini Tharmaratnam, Daniel Oberski, Hemant Ishwaran, Dawn K Wilson, and M Lee Van Horn. Identification of predicted individual treatment effects in randomized clinical trials. *Statistical methods in medical research*, page 0962280215623981, 2016.

[34] Patrick M Schnell, Qi Tang, Walter W Offen, and Bradley P Carlin. A bayesian credible subgroups approach to identifying patient subgroups with positive treatment effects. *Biometrics*, 72(4):1026–1036, 2016.

[35] Nicolás M. Ballarini, Gerd K. Rosenkranz, Thomas Jaki, Franz König, and Martin Posch. Subgroup identification in clinical trials via the predicted individual treatment effect. *PLOS ONE*, 13(10):1–22, 10 2018.

[36] Stirling Chow and Frank Ruskey. Towards a general solution to drawing area-proportional euler diagrams. *Electronic Notes in Theoretical Computer Science*, 134:3–18, 2005.

[37] Peter Rodgers, Jean Flower, Gem Stapleton, and John Howse. Drawing area-proportional venn-3 diagrams with convex polygons. In *Diagrams*, pages 54–68. Springer, 2010.

[38] Luana Micallef and Peter Rodgers. eulerape: drawing area-proportional 3-venn diagrams using ellipses. *PloS one*, 9(7):e101717, 2014.

[39] Hanbo Chen. *VennDiagram: Generate High-Resolution Venn and Euler Plots*, 2018. R package version 1.6.20.

[40] Angus Johnson and Adrian Baddeley. *polyclip: Polygon Clipping*, 2018. R package version 1.9-0.

[41] Edzer J. Pebesma and Roger S. Bivand. Classes and methods for spatial data in R. *R News*, 5(2):9–13, November 2005.

[42] Roger Bivand and Colin Rundel. *rgeos: Interface to Geometry Engine - Open Source ('GEOS')*, 2018. R package version 0.3-28.

[43] Jonathan Swinton. *Venn diagrams in R with the Vennerable package*, 2009. R package version 3.1.0.9000.

[44] Henry Heberle, Gabriela Vaz Meirelles, Felipe R da Silva, Guilherme P Telles, and Rosane Minghim. Interactivenn: a web-based tool for the analysis of sets through venn diagrams. *BMC bioinformatics*, 16(1):169, 2015.

[45] Harris Cooper, Larry V Hedges, and Jeffrey C Valentine. *The handbook of research synthesis and meta-analysis*. Russell Sage Foundation, 2009.

[46] Jack Cuzick. Forest plots and the interpretation of subgroups. *The Lancet*, 365(9467):1308, 2005.

[47] Doron Aronson. Subgroup analyses with special reference to the effect of antiplatelet agents in acute coronary syndromes. *Thrombosis and haemostasis*, 112(01):16–25, 2014.

[48] Hadley Wickham. *ggplot2: elegant graphics for data analysis*. Springer, 2016.

[49] Ilya Lipkovich and Alex Dmitrienko. Strategies for identifying predictive biomarkers and subgroups with enhanced treatment effect in clinical trials using sides. *Journal of biopharmaceutical statistics*, 24(1):130–153, 2014.

[50] Heidi Seibold, Achim Zeileis, and Torsten Hothorn. Model-based recursive partitioning for subgroup analyses. *The international journal of biostatistics*, 12(1):45–63, 2016.

[51] RF Galbraith. A note on graphical presentation of estimated odds ratios from several clinical trials. *Statistics in medicine*, 7(8):889–894, 1988.

[52] RF Galbraith. Graphical display of estimates having differing standard errors. *Technometrics*, 30(3):271–281, 1988.

[53] Krintan A L'Abbé, Allan S Detsky, and Keith O'rourke. Meta-analysis in clinical research. *Annals of internal medicine*, 107(2):224–233, 1987.

[54] Marco Bonetti and Richard D Gelber. Patterns of treatment effects in subsets of patients in clinical trials. *Biostatistics*, 5(3):465–481, 2004.

[55] Marco Bonetti and Richard D Gelber. A graphical method to assess treatment-covariate interactions using the cox model on subsets of the data. *Statistics in medicine*, 19(19):2595–2609, 2000.

[56] Willi Sauerbrei, Patrick Royston, and Karina Zapien. Detecting an interaction between treatment and a continuous covariate: A comparison of two approaches. *Computational statistics & data analysis*, 51(8):4054–4063, 2007.

[57] Carl Edward Rasmussen and Christopher KI Williams. *Gaussian processes for machine learning*, volume 1. MIT press Cambridge, 2006.

[58] Alexander Lex, Nils Gehlenborg, Hendrik Strobelt, Romain Vuillemot, and Hanspeter Pfister. Upset: visualization of intersecting sets. *IEEE transactions on visualization and computer graphics*, 20(12):1983–1992, 2014.

[59] Nils Gehlenborg. *UpSetR: A More Scalable Alternative to Venn and Euler Diagrams for Visualizing Intersecting Sets*, 2017. R package version 1.3.3.

[60] Martin Krzywinski, Jacqueline Schein, Inanc Birol, Joseph Connors, Randy Gascoyne, Doug Horsman, Steven J Jones, and Marco A Marra. Circos: an information aesthetic for comparative genomics. *Genome research*, 19(9):1639–1645, 2009.

[61] Zuguang Gu, Lei Gu, Roland Eils, Matthias Schlesner, and Benedikt Brors. circlize implements and enhances circular visualization in r. *Bioinformatics*, 30:2811–2812, 2014.

[62] Florence Nightingale. *Notes on matters affecting the health, efficiency, and hospital administration of the British army: founded chiefly on the experience of the late war*. Harrison and Sons, 1858.

[63] Michal Bojanowski and Robin Edwards. *alluvial: R Package for Creating Alluvial Diagrams*, 2016. R package version: 0.1-2.

[64] Karline Soetaert. *diagram: Functions for Visualising Simple Graphs (Networks), Plotting Flow Diagrams*, 2017. R package version 1.6.4.

[65] William S Cleveland and Robert McGill. Graphical perception and graphical methods for analyzing scientific data. *Science*, 229(4716):828–833, 1985.

[66] Ilya Lipkovich, Alex Dmitrienko, Christoph Muysers, and Bohdana Ratitch. Multiplicity issues in exploratory subgroup analysis. *Journal of biopharmaceutical statistics*, 28(1):63–81, 2018.

[67] Björn Bornkamp, David Ohlssen, Baldur P Magnusson, and Heinz Schmidli. Model averaging for treatment effect estimation in subgroups. *Pharmaceutical statistics*, 16(2):133–142, 2017.

[68] Ravi Varadhan and Sue-Jane Wang. Standardization for subgroup analysis in randomized controlled trials. *Journal of biopharmaceutical statistics*, 24(1):154–167, 2014.

[69] Heike Hofmann. Exploring categorical data: interactive mosaic plots. *Metrika*, 51(1):11–26, 2000.

[70] Bodo Kirsch, Susanne Lippert, Thomas Schmelter, Christoph Muysers, and Hermann Kulmann. *subscreen: Systematic Screening of Study Data for Subgroup Effects*, 2018. R package version 1.0.0.

[71] Winston Chang, Joe Cheng, JJ Allaire, Yihui Xie, and Jonathan McPherson. *shiny: Web Application Framework for R*, 2018. R package version 1.1.0.

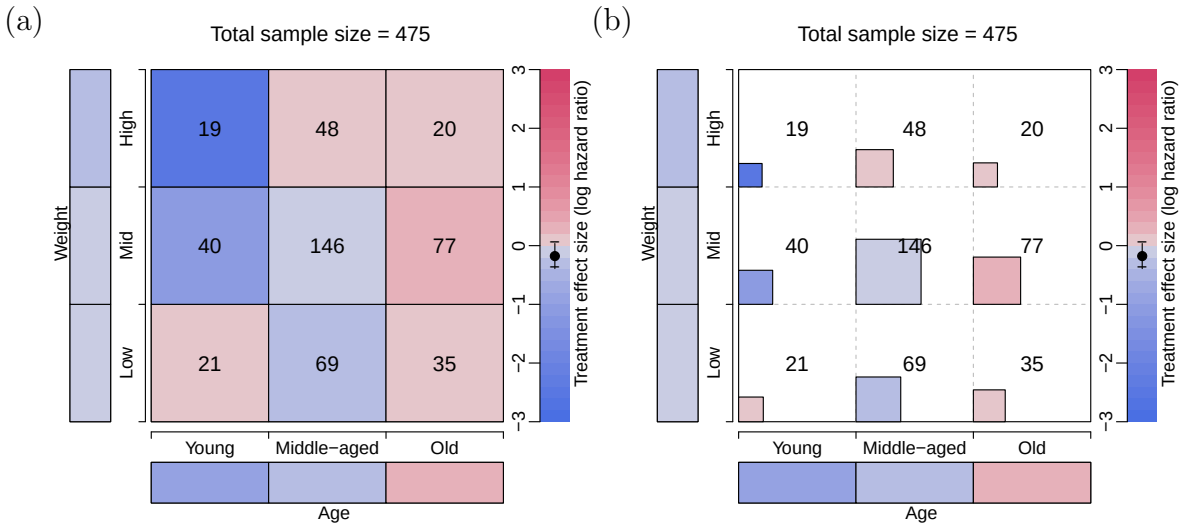

Figure 1: Level plots of treatment effect in terms of the log-hazard ratio across mutually disjoint subgroups defined by age and weight categorised in three levels. The cells on the bottom and the left margins correspond to the marginal subgroups defined by the levels of age and weight. In (b), the area of each square inside the cells is proportional to the sample sizes, which are also displayed in the middle of the cells.

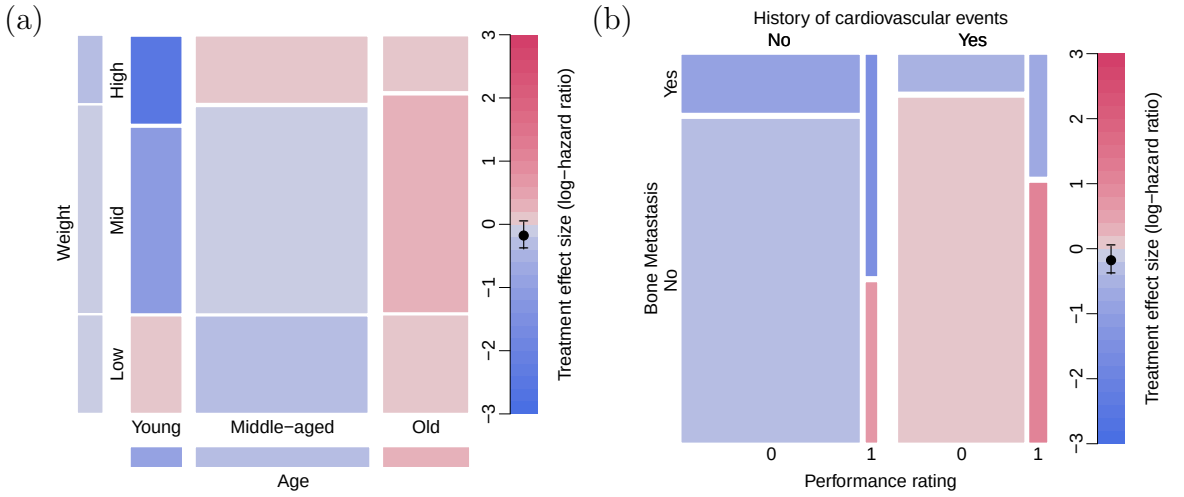

Figure 2: (a) Mosaic plot of treatment effect in terms of the log-hazard ratio across mutually disjoint subgroups defined by age and weight categorised in three levels. The cells on the bottom and the left margins correspond to the marginal subgroups defined by the levels of age and weight. The area of each mosaic is proportional to the sample sizes. (b) Mosaic plot of treatment effect in terms of the log-hazard ratio across mutually disjoint subgroups defined by history of cardiovascular events, performance rating and bone metastasis.

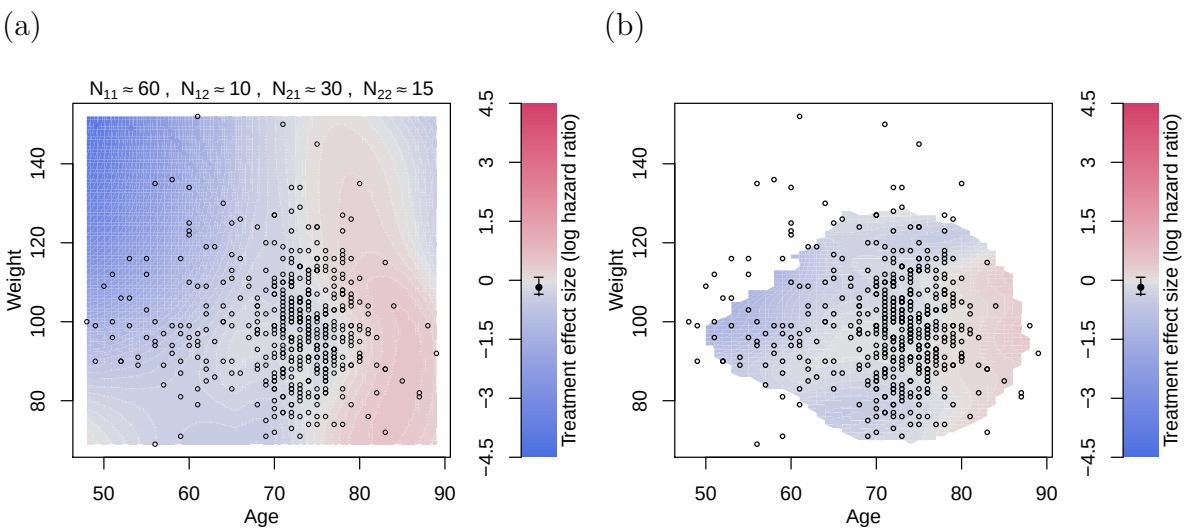

Figure 3: Contour plot of treatment effect in terms of the log-hazard ratio over the plane of age and weight. (a) Contour lines are drawn by forming subgroups with neighbouring subjects, calculating the treatment effect for subgroups and interpolating the results using loess. N_{11} stands for the sample size of a marginal subgroup defined by a range of age, N_{12} is the overlap size of the immediate marginal subgroups on age, N_{21} is the sample size of the subset of a marginal subgroup on age but further defined by a range of weight, and N_{22} is the overlap size of the immediate subgroups (which are the subset of a marginal subgroup on age) on weight. (b) Contour lines are drawn by fitting a local regression at each point of the grid, using subjects weights according to their distance to the point of the grid. Points with few subjects in the vicinity of the grid point were left blank

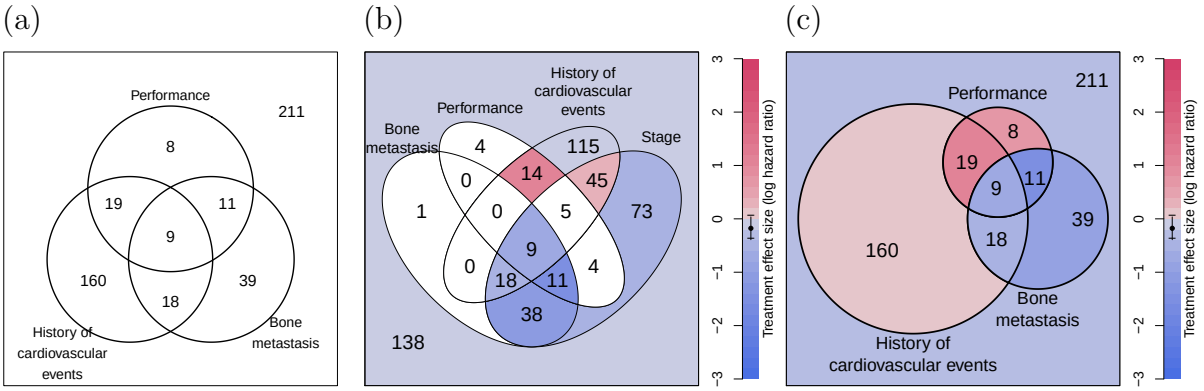

Figure 4: (a) Venn diagram of 3 subgroups defined by presence of bone metastasis, history of cardiovascular events, and performance rating = 1. (b) Venn diagram of 4 sets defined by presence of bone metastasis, disease stage, performance rating = 1 and history of cardiovascular events with treatment effect sizes in terms of the log-hazard ratios. (c) Approximate area-proportional Venn diagram of 3 subgroups defined by presence bone metastasis, history of cardiovascular events and performance rating = 1 with treatment effect sizes in terms of the log-hazard ratios.

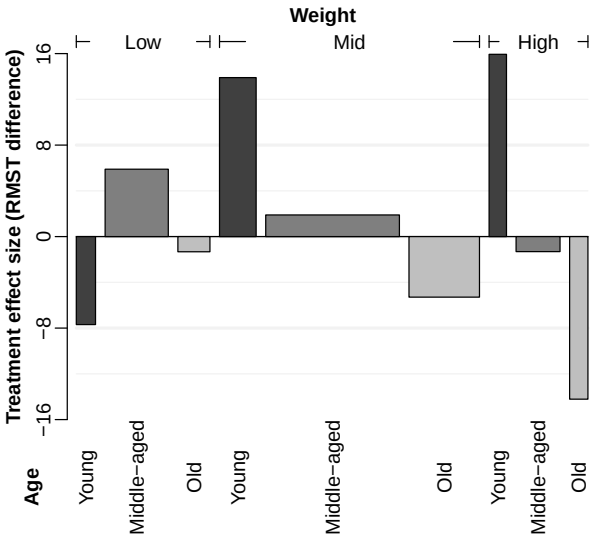

Figure 5: Bar plot of treatment effect in terms of the difference in restricted mean survival time across mutually disjoint subgroups defined by age and weight categorised in three levels. The width of each bar is proportional to the sample size for subgroups. The area can be interpreted as the gain/loss in restricted mean survival when using treatment in comparison to control. Black, grey and light grey indicate the age categories young, middle-aged and old, respectively.

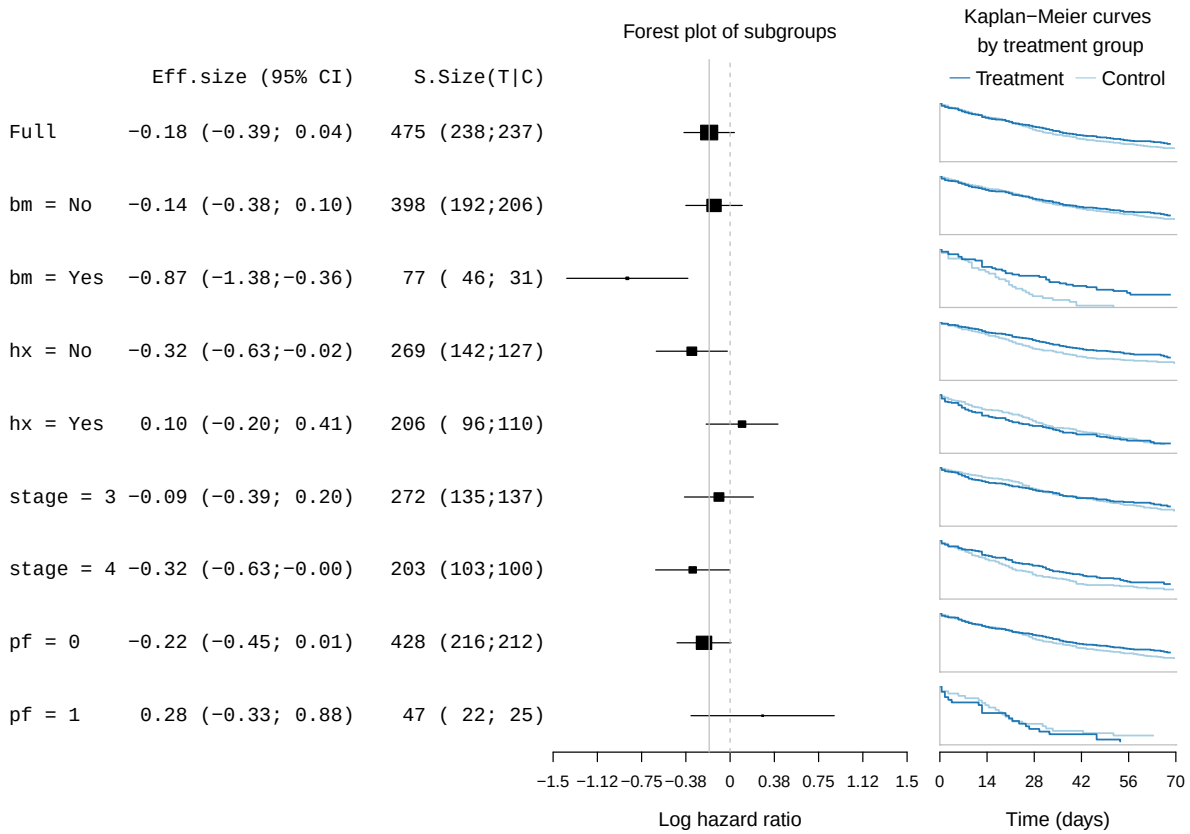

Figure 6: Forest plot for subgroups defined by performance (pf), stage, history of cardiovascular events (hx) and existence of bone metastasis (bm). Effect sizes in terms of the log-hazard ratio and associated treatment and control group Kaplan-Meier curves are displayed.

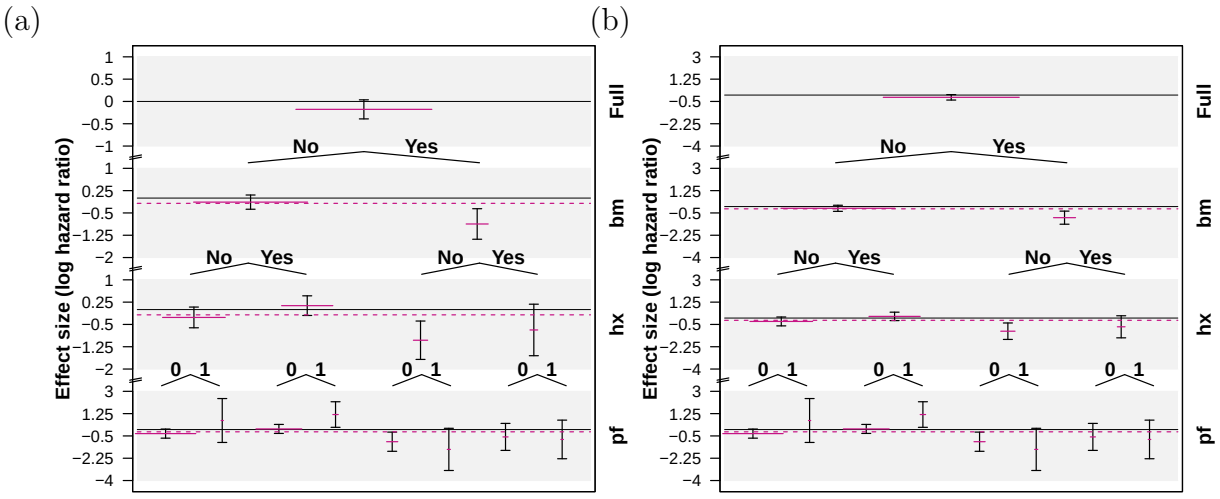

Figure 7: Tree plot for the treatment effect in terms of the log-hazard ratio for subgroups defined by category combinations of existence of bone metastasis (bm), history of cardiovascular events (hx), and performance rating (pf). Each layer shows the 95% C.I. of treatment effect differences for the associated subgroups. The purple horizontal lines placed in the middle of C.I. have a length proportional to the weight of subgroup sample size over the full population. In (a) the y-axes are independent in each layer of the plot, while in (b) y-axes are kept fixed across levels, which allows comparing variability in the estimates

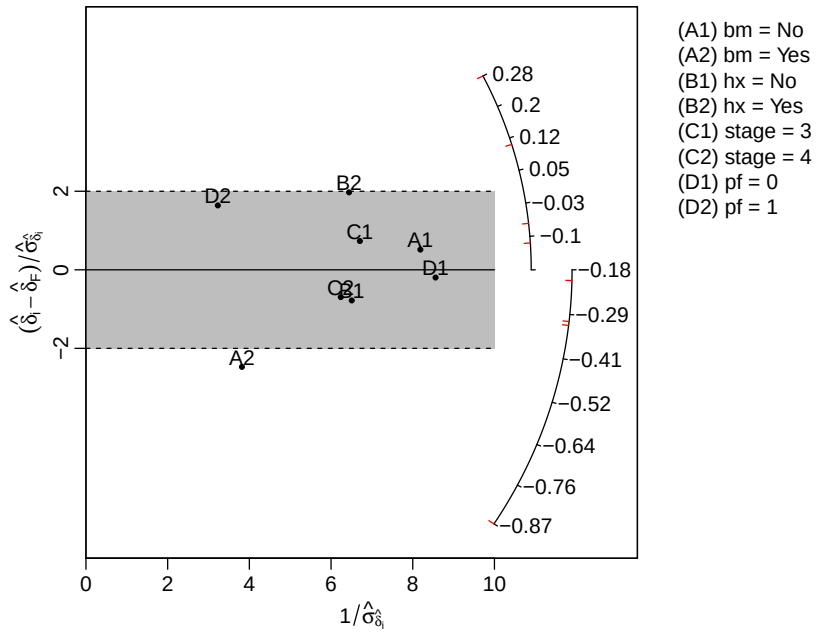

Figure 8: Galbraith plot for subgroups defined by existence of bone metastasis (bm), history of cardiovascular events (hx), stage, and performance rating (pf).

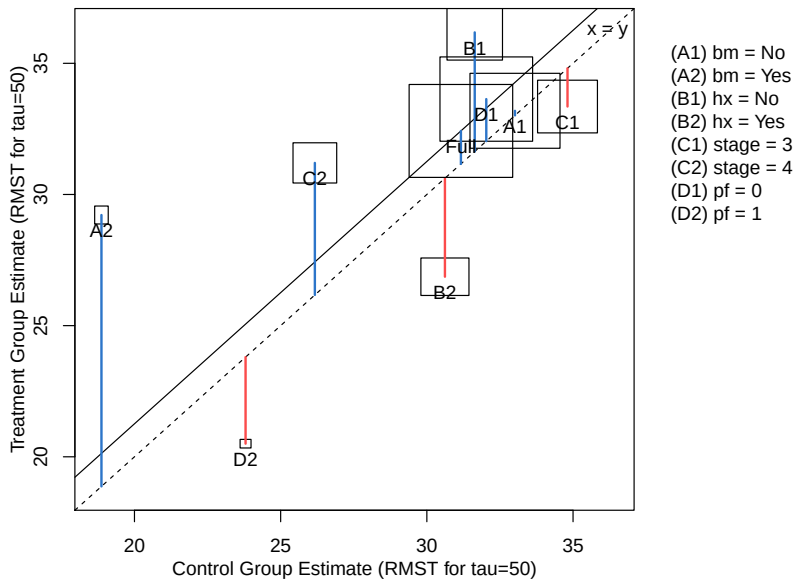

Figure 9: L'Abbé plot for subgroups defined by performance (pf), stage, history of cardiovascular events (hx) and existence of bone metastasis (bm). Effect sizes are given in terms of the difference in restricted mean survival time (RMST).

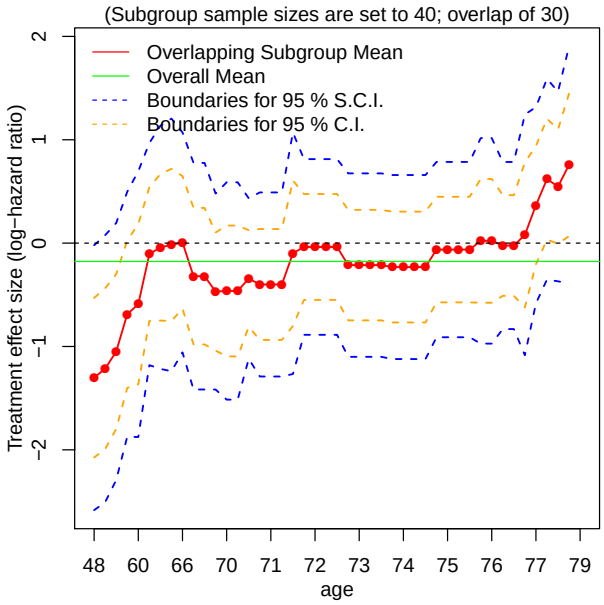

Figure 10: STEPP plot of overlapping subgroups defined by age. Each subgroup has a sample size of around 40 (N11 = 40) and is controlled to have about 87% (N12/N11) being overlapped with the neighbouring subgroups.

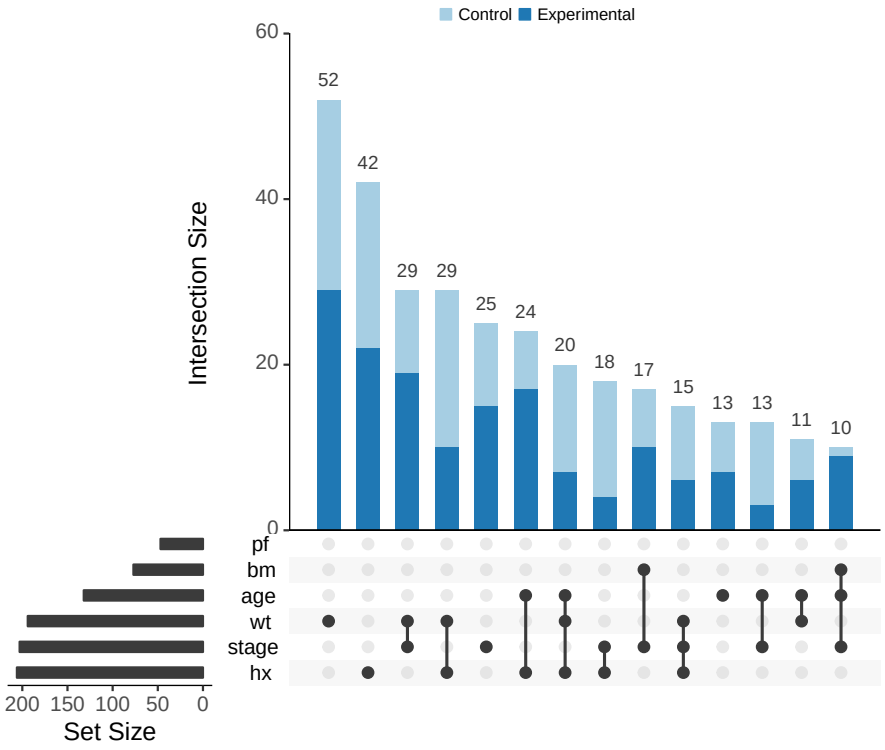

Figure 11: Upset plot displaying the subgroups conformed by the intersection of all subgroup-defining covariates

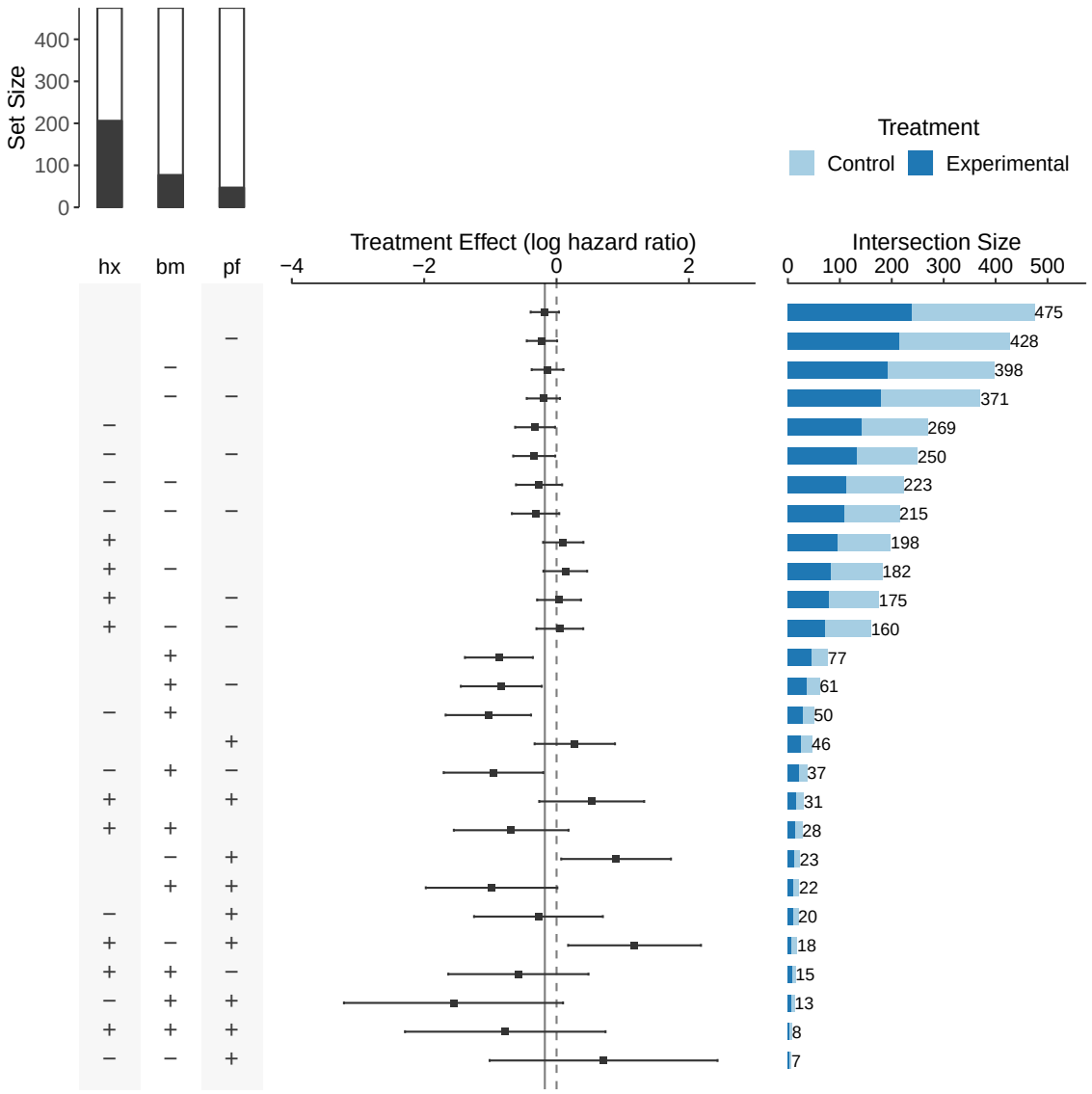

Figure 12: Improved UpSet plot for subgroups defined by performance (pf), bone metastasis (bm) and history of cardiovascular events (hx). The panel on the left (matrix) displays how the subgroups are formed by assigning a '+' if the variable is equal to 1 and a '−' if the variable is equal to 0. The bar plot on top of the matrix panel indicates the marginal set sizes in relation to the total sample size, with the black region corresponding to the 1 or 'yes' category and the white region corresponding to the 0 or 'no' category. Treatment effect sizes and their confidence intervals are displayed in the panel on the middle and the subgroup sizes in the horizontal bar plot on the right.

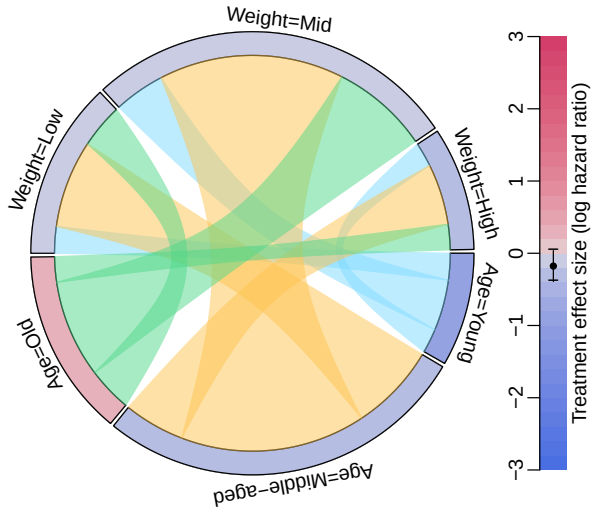

Figure 13: Chord diagram for the subgroups formed by age and weight. The colours along the circle represent the treatment effect in terms of the log-hazard ratio. The ribbons that link the subgroups represent their overlap.

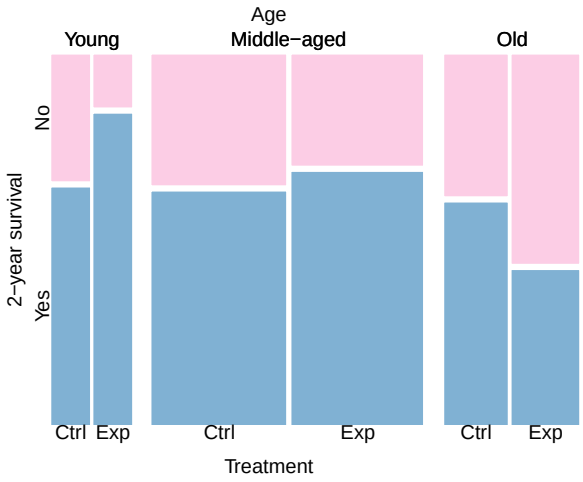

Figure 14: Mosaic plot displaying 2-year survival by treatment arm for the subgroups formed by age categories.

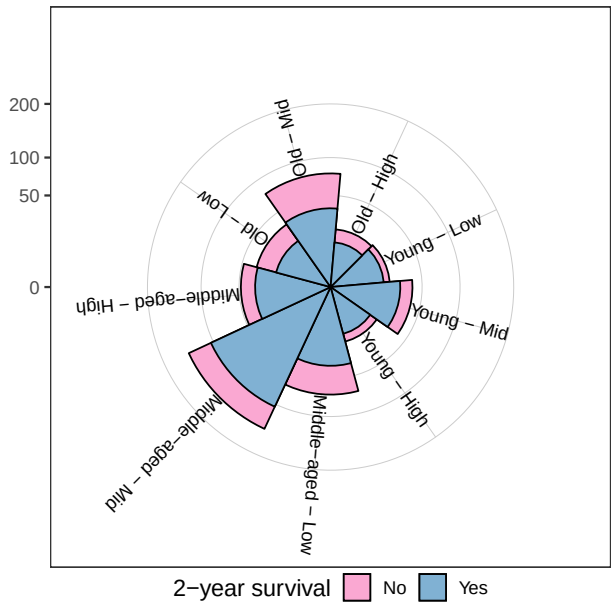

Figure 15: Nightingale coxcombs plot for subgroups defined by age and weight with 2-year survival rate. The radius of the sectors are proportional to the square root of the sample sizes in the subgroups

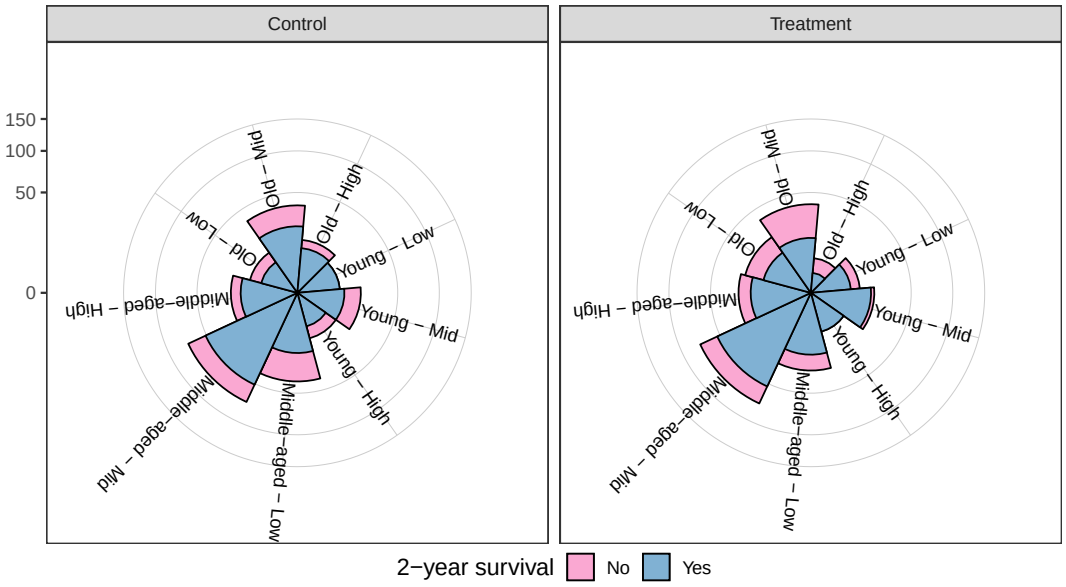

Figure 16: Nightingale coxcombs plot for subgroups defined by age and weight with 2-year survival rate and separated by treatment arm. The radius of the sectors are proportional to the square root of the sample sizes in the subgroups

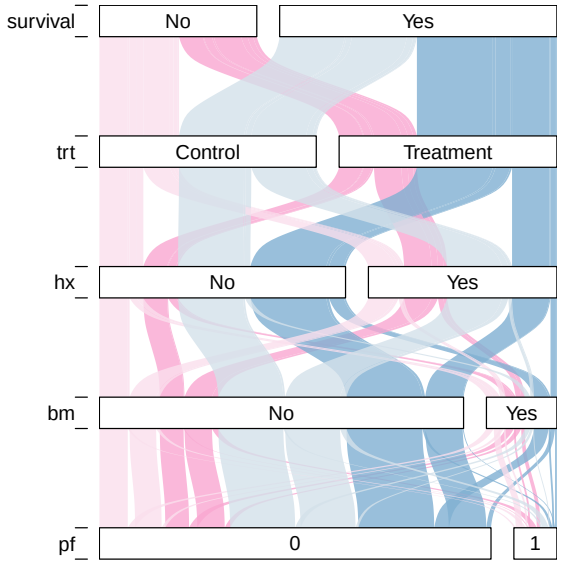

Figure 17: Alluvial diagram displaying the distribution of patients across the subgroups defined by history of cardiovascular events (hx), existence of bone metastasis (bm) and performance rating (pf). The dark bands correspond to patients that were randomised to treatment while lighter ones to patients in control. Blue coloured bands represent patients that had survived for at least 2 years, while pink ones represent those who did not. The width of the bands is proportional to the sizes of the subgroups.

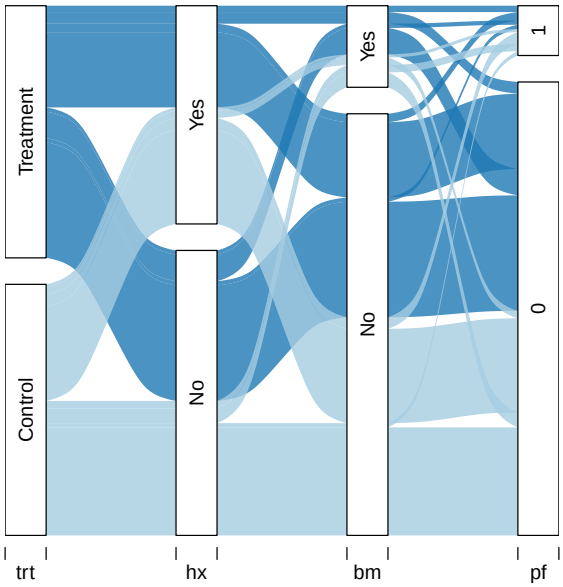

Figure 18: Alluvial diagram displaying the distribution of patients across the subgroups defined by history of cardiovascular events (hx), existence of bone metastasis (bm) and performance rating (pf). The dark blue bands correspond to patients that were randomised to treatment while light blue ones to patients in control. The width of the bands is proportional to the sizes of the subgroups.

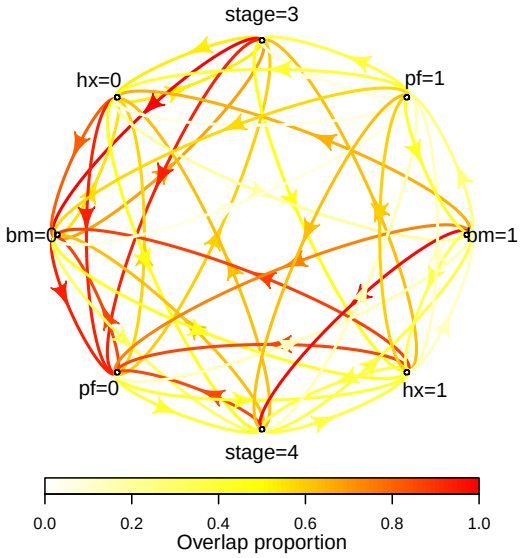

(a) Line plot with bidirectional arrowed curves for relative overlap proportions for pairwise subgroups.

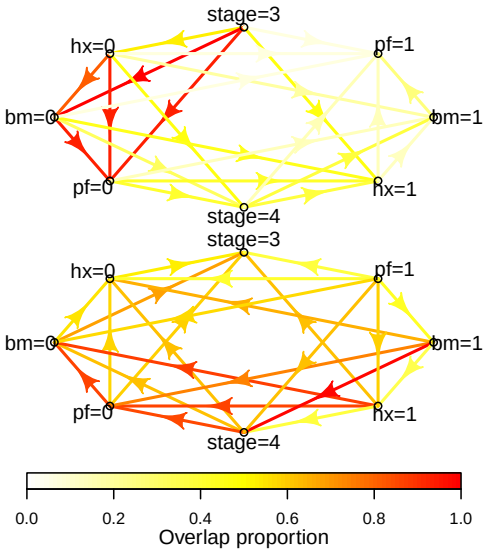

(b) Line plots with unidirectional arrowed lines for relative overlap proportions for pairwise subgroups.

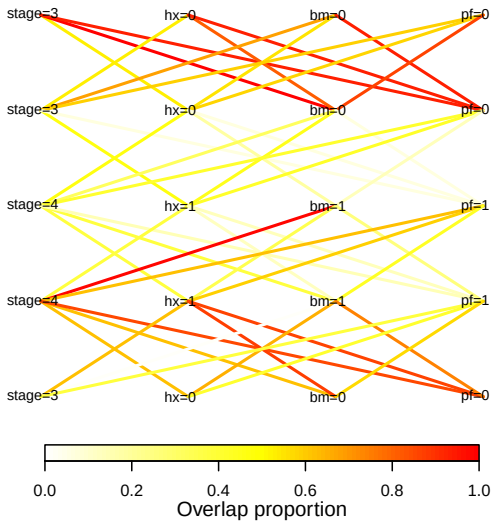

(c) Line plot for relative overlap proportions for pairwise subgroups.

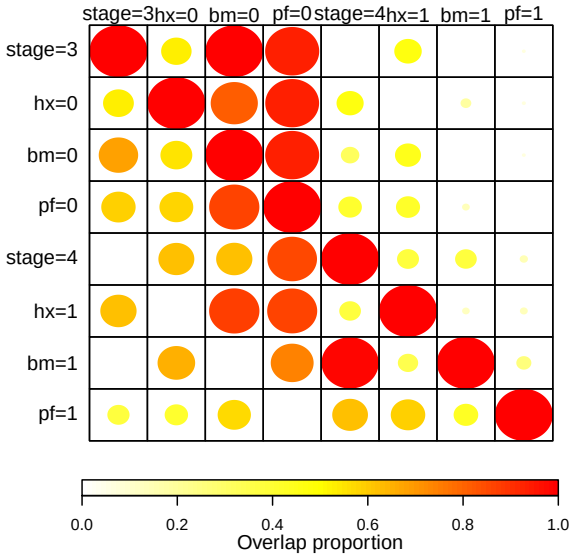

(d) Matrix plot for relative overlap proportions for pairwise subgroups.

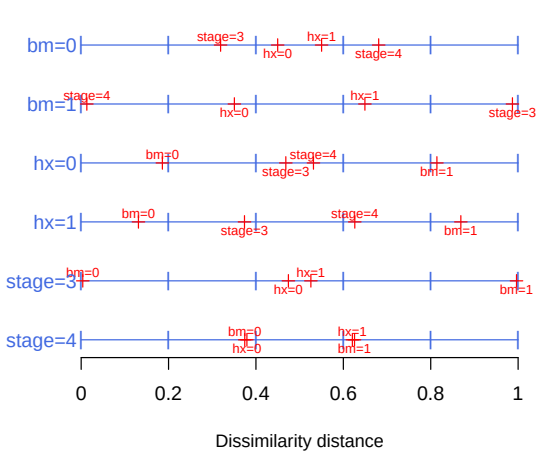

(e) Dissimilarity measures for marginal subgroups.

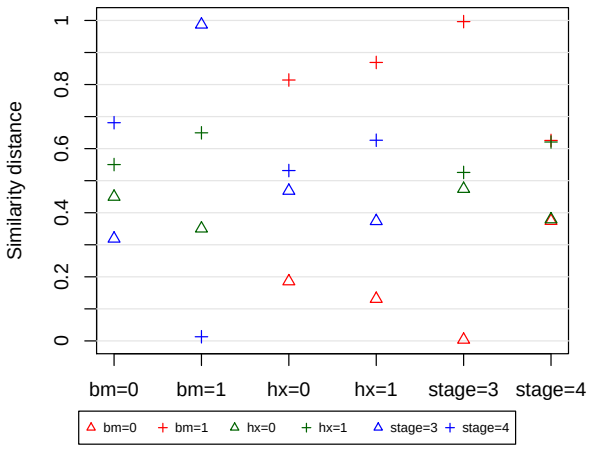

(f) Dot plot for dissimilarity measures for marginal subgroups.

Figure 19: Plots for subgroup information about pairwise overlap proportions or dissimilarity measure.